PALEOCEANOGRAPHY, VOL. 21, PA4101, doi:10.1029/2006PA001306, 2006

Click Here for Full Article

Promotion of meridional overturning by Mediterranean-derived salt during the last deglaciation

M. Rogerson,[1] E. J. Rohling,[2] and P. P. E Weaver[2]

Received 20 April 2006; revised 11 July 2006; accepted 19 July 2006; published 4 November 2006.

[1] We demonstrate that changes in the behavior of the Mediterranean Outflow Water (MOW) prior to and through the last deglaciation played an important role in promoting Meridional Overturning Circulation (MOC). Estimation of past MOW salt and heat fluxes indicates that they gradually increased through the last deglaciation. Between 17.5 and 14.6 thousand years ago (ka B.P., where B.P. references year 1950), net evaporation from the Mediterranean exported sufficient fresh water from the North Atlantic catchment to cause an average salinity increase of 0.5 psu throughout the upper 2000 m of the entire North Atlantic to the north of 25°N. Combined with rapid intensification and shoaling of the MOW plume, which we identify around 15–14.5 ka B.P., this deglacial MOW-related salt accumulation preconditioned the North Atlantic for abrupt resumption of the MOC at 14.6 ka B.P.

Citation: Rogerson, M., E. J. Rohling, and P. P. E. Weaver (2006), Promotion of meridional overturning by Mediterranean-derived salt during the last deglaciation, *Paleoceanography*, *21*, PA4101, doi:10.1029/2006PA001306.

1. Introduction

[2] North Atlantic circulation changes have played a key role in climate change during the last deglaciation (18–10 ka B.P.) [*Boyle*, 2000; *McManus et al.*, 2004]. Most notable was the abrupt increase in strength of the MOC at the onset of the Bölling warm period (14.6 ka B.P.) [*Gherardi et al.*, 2005; *McManus et al.*, 2004]. The associated increase in oceanic poleward heat advection is thought to underlie rapid high-latitude warming [*McManus et al.*, 2004]. Accelerated glacial retreat due to this warming, however, ought to have increased the supply of meltwater to downwelling regions, with negative impacts on the MOC [*Schmidt et al.*, 2004]. Salt advection from the Caribbean [*Schmidt et al.*, 2004] and Indian Ocean [*Knorr and Lohmann*, 2003] has been proposed as a density amplification mechanism that maintained the MOC during glacial retreat [*Schmidt et al.*, 2004]. It has also been suggested [*Rahmstorf*, 1998; *Reid*, 1979] that the saline plume of MOW, which today affects the eastern North Atlantic around 1000 m depth, is capable of providing density amplification promoting MOC, though no evidence in support of this has been previously presented.

[3] During the last glaciation, global sea level stood about 120 m lower than today [*Fairbanks*, 1989], which restricted water mass exchange between the Mediterranean and the Atlantic through the narrow (13.7 km) and shallow (284 m) Strait of Gibraltar. This caused a roughly twofold increase in the salinity contrast between Mediterranean and Atlantic waters relative to the present [*Matthiesen and Haines*, 2003; *Rohling and Bryden*, 1994]. Such a great salinity difference at Gibraltar (ΔS_{gib}), combined with a reduced volume of Mediterranean Outflow through the Strait of Gibraltar, resulted in a smaller and denser MOW plume that settled to greater depth within the Atlantic [*Rogerson et al.*, 2005]. This caused the formation of a deep glacial sediment drift on the northern margin of the Gulf of Cadiz (GoC) [*Rogerson et al.*, 2005], as well as changes in sedimentation and $\delta^{13}C$ of benthic foraminifera at ~2000 m on the Tejo Plateau (Portuguese Margin; see Figure 1) [*Schönfeld and Zahn*, 2000].

[4] The observations of MOW activity around 2000 m water depth during the Last Glacial Maximum (LGM) place it at about twice its modern settling depth of ~1000 m [*O'Neill-Baringer and Price*, 1999]. If we assume that the observations on the Tejo plateau [*Schönfeld and Zahn*, 2000] characterize the base of the MOW rather than its core, then a minimum estimate of ~500 m (relative to the present) can be derived for glacial deepening of the MOW plume. Given the reduced overall transport in the plume [*Rogerson et al.*, 2005], even that minimum estimate would place the top of the glacial MOW plume considerably below 1000 m water depth, in agreement with the absence of evidence for glacial flow on the upper GoC slope [*Nelson et al.*, 1993; *Stow et al.*, 1986] (Figure 1a).

[5] Here we present data for 5 cores from the Gulf of Cadiz, supported by data for 5 additional cores from the literature, to reconstruct changes in the MOW plume's settling depth through the last deglaciation. Additionally, we use physical arguments to derive quantitative estimates of the impact of MOW salt and heat fluxes on the North Atlantic during the same period.

2. Methods

[6] Ten cores from the Gulf of Cadiz (see Table 1) containing sediment records across the last deglaciation span a range of water depths relative to the modern MOW (see Figures 1 and 2). The deep water (>1000 m

[1]Geography Department, University of Hull, Hull, UK.
[2]National Oceanography Centre, Southampton, Southampton, UK.

0883-8305/06/2006PA001306$12.00

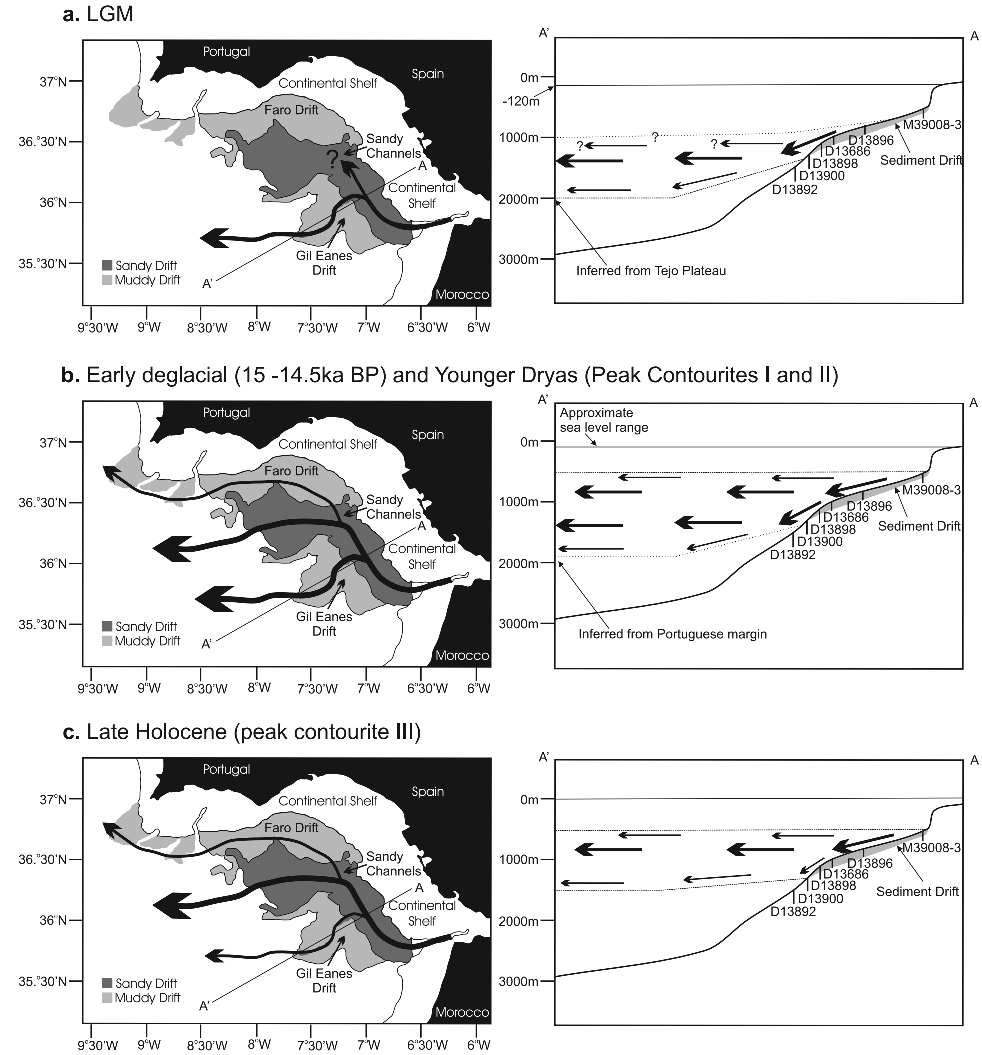

Figure 1. Recent, deglacial, and LGM positions of the Mediterranean Outflow within the Gulf of Cadiz. (left) Sections are shown on (right) corresponding maps. Position of relevant cores is shown on sections.

water depth) part of the sediment drift is represented by D13898 (1111 m) and D13900 (1297 m) positioned on the lower Gil Eanes Drift. Core D13892 (1497 m) is positioned in the central Gulf of Cadiz, beyond the sediment drift. The MOW does not interact with the sea floor directly in this area, but is an important source of fine clastic sediment [*Rogerson et al.*, 2006]. Intermediate depths (1000–700 m) are represented by cores D13896 (817 m) and D13686 (998 m) on the upper Gil Eanes Drift. The shallow (<800 m depth) part of the system is represented by 5 representative published core records. Kc8227 (615 m) [*Stow et al.*, 1986] from the Faro Drift and M39008-3 (557 m) [*Heilemann*, 2000; *Schönfeld*, 2002] from a terrace in the "sandy channels" region (Figure 2) exhibit a stratigraphy typical of cores from sediment drifts on the upper slope. Three additional sediment cores (designated here as N1-N3, all between 500 and 600 m water depth) are positioned within the part of the slope that is today affected by the core of the MOW [*Nelson et al.*, 1993] (the "Sandy Channels" region on Figure 2a).

[7] Timeframes for cores from the Gil Eanes Drift (D13686, D13892, D13896, D13898 and D13900) are constrained by 19 previously published [*Rogerson et al.*, 2005] and 8 new Accelerator Mass Spectrometry (AMS) ^{14}C datings (see Table 2). These radiocarbon datings were measured on hand-picked planktonic foraminifera (excluding deep-dwelling taxa such as the genus *Globorotalia*).

Table 1. Location Information for Cores Reported in This Study

Core Name	Latitude	Longitude	Water Depth, m
D13686	35°51′	7°11′	998
D13892	35°47′	7°43′	1497
D13896	36°03′	7°18′	817
D13898	35°54′	7°25′	1111
D13900	35°49′	7°31′	1297
M39008-3	36°23′	7°04′	557
Kc8227	36°42′	7°57′	619
N-1	36°49′	7°35′	~500
N-2	36°00	6°52′	~500
N-3	36°15′	7°16′	~600

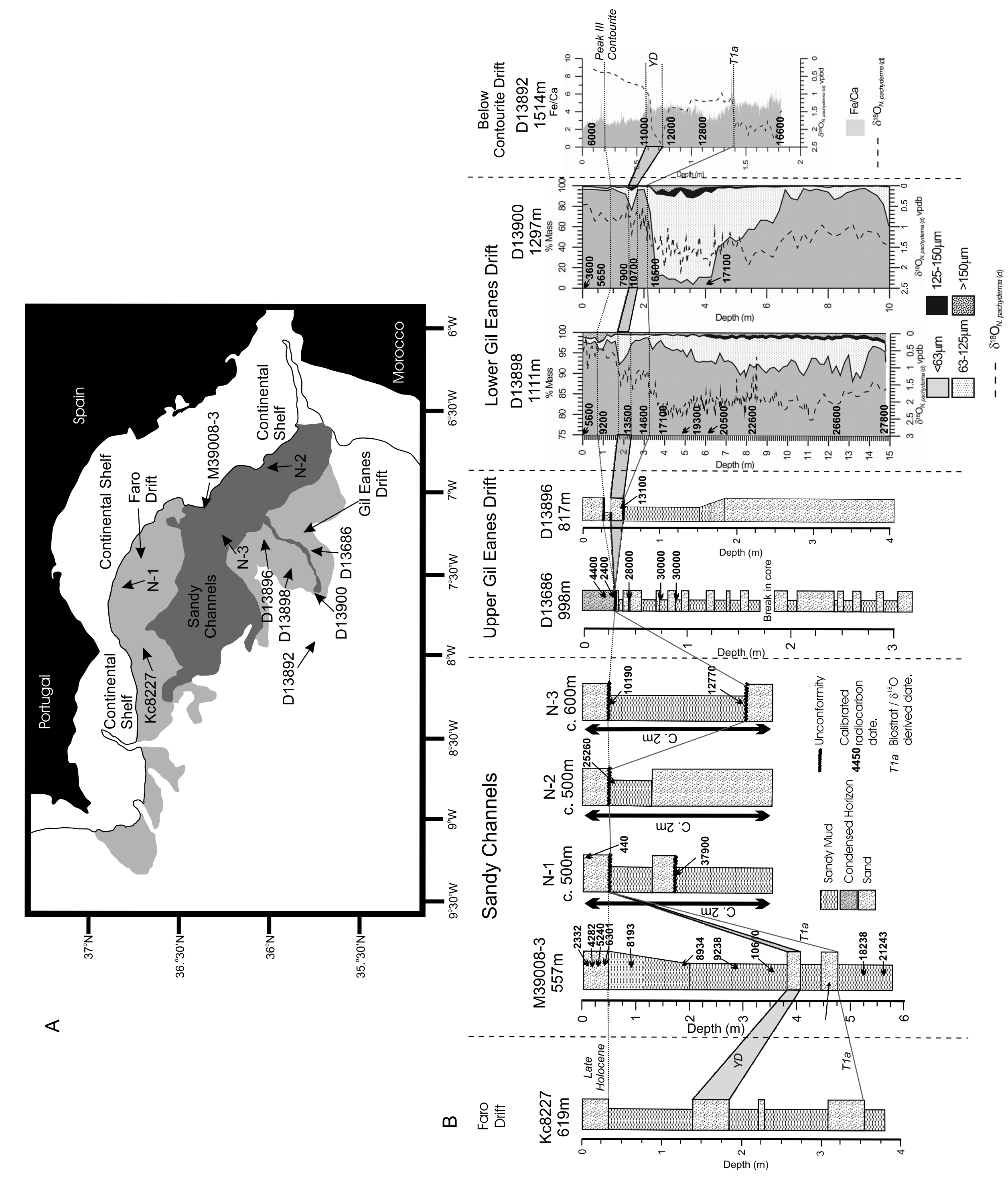
A
Portugal
Spain
Morocco
Continental Shelf
Faro Drift
Sandy Channels
Gil Eanes Drift
M39008-3
Kc8227
N-1
N-2
N-3
D13686
D13892
D13896
D13898
D13900
B
Faro Drift
Kc8227 619m
Sandy Channels
M39008-3 557m
N-1 c. 500m
N-2 c. 500m
N-3 c. 600m
Upper Gil Eanes Drift
D13686 998m
D13896 817m
Lower Gil Eanes Drift
D13898 1111m
D13900 1297m
Below Contourite Drift
D13892 1514m
Depth (m)
Sandy Mud
Condensed Horizon
Sand
Unconformity
Calibrated radiocarbon date.
Biostrat / δ18O derived date.
Break in core
Late Holocene
YD
T1a
Peak III Contourite
Fe/Ca
% Mass
<63μm
63-125μm
125-150μm
>150μm

Figure 2

Table 2. New AMS^{14}C Datings for Cores From the Gil Eanes Drift[a]

Core	Depth, cm	Conventional Age	Calibrated Age	Laboratory Sample Code
D13900	0	4390 ± 30 B.P.	3600	KIA 27016
D13900	59	6330 ± 35 B.P.	5650	KIA 27017
D13900	151	8475 ± 40 B.P.	7900	KIA 27018
D13900	173	10245 ± 50 B.P.	10700	KIA 27019
D13900	233	14780 ± 80 B.P.	16500	KIA 27020
D13900	402	15400 ± 90 B.P.	17100	KIA 27021
D13686	32	3490 ± 30 B.P.	2400	KIA 27014
D13896	31	12340 ± 70 B.P.	13100	KIA 27015

[a]Calibration of dates is done using the OxCal program assuming a 400 years reservoir age.

The analyses were undertaken via the NERC Radiocarbon Laboratory (NERC-RCL) at the University of Arizona NSF-AMS facility and converted to calendar age using the OxCal program (http://www.rlaha.ox.ac.uk/O/oxcal.php?group=O). In the case of the dates older than 26 ka B.P., the Bard et al polynomial calibration [*Bard et al.*, 1998] has been used. Core M39008-3 has been separately dated with 10 AMS^{14}C analyses [*Cacho et al.*, 2001; *Schönfeld*, 2002] (Figure 2b). The age control on records obtained from the work of Nelson is based on 5 AMS^{14}C datings [*Nelson et al.*, 1993].

[8] Correlation of the core records presented is based in the first instance on the ^{14}C timescales, then fine-tuned by correlation of regional events in the planktonic foraminiferal assemblage and $\delta^{18}O_{\text{planktonic foraminifera}}$ records [*Rogerson et al.*, 2005]. For foraminiferal assemblage, stable isotope and ^{14}C analyses, samples were disaggregated, washed and sieved to remove all material finer than 150 μm, using demineralized water. All specimens selected for stable isotope analyses were washed and sonicated in methanol to remove surface contamination. Analyses were carried out on 7–15 individuals of *Neogloboquadrina pachyderma* (d) between sizes of 150 and 212 μm. Stable isotope analyses were carried out using a Europa Geo 2020 mass spectrometer with individual acid dosing. The stable carbon and oxygen isotope ratios are expressed as δ values, in per mil (‰), relative to the Vienna Peedee Belemnite standard [*Coplen*, 1994].

[9] Rough grain size information was obtained by weighing a set of subsamples and then sieving these at 63, 125 and 150 μm, weighing the residues to determine the percentage weight of four grain size fractions (<63 μm, 63–125 μm, 125–150 μm and >150 μm). Here, we assume that changes in the balance of sediment coarser and finer than 63 μm are representative of changes in local energy and/or sediment transport conditions. However, in the light of discussion on the use of quantitative paleovelocity proxies based on grain size data by [*Weltje and Prins*, 2003] and the position of many of our cores adjacent to contourite channels, we to not venture a quantitative paleovelocity reconstruction in this paper. Bulk chemical analysis was performed for core D13892 at a down core resolution of 400 μm, using the Cox Analytical Systems Itrax XRF core logger at the National Oceanography Centre, Southampton, UK. We present only Fe/Ca data here, which we interpret as being representative of the balance of the detrital and carbonate phases in the sediment [*Rogerson et al.*, 2006].

[10] Water mass exchange transports through the Strait of Gibraltar have been calculated based on a hydraulic control model in combination with mass and salt conservation statements [*Bryden and Kinder*, 1991], according to

$$Q_{net} = C\frac{W_s D_s}{2}\sqrt{\frac{g\beta\Delta SD_s}{\rho_{med}}} = \frac{2S_{atl} + \Delta S_{gib}}{\Delta S_{gib}}X_{med} \qquad (1)$$

where Q_{net} determines the net exchange across the sill ($Q_{atl} - Q_{med}$), W_s and D_s are the width and depth at the sill, C is a constant depending on sill geometry (0.28), g = 9.81 m s^{-2}, and β is a coefficient used to convert $\Delta\rho_{gib}$ to ΔS_{gib} (0.77 $\times$ 10^{-3} g cm^{-3} ppt^{-1}) [*Bryden and Kinder*, 1991]. S represents salinity, X represents net evaporation and *atl* and *med* represent properties of Atlantic and Mediterranean water respectively. Volume flux and ΔS_{gib} estimates are taken from an existing model for the Gibraltar exchange exploiting this relationship [*Bryden and Kinder*, 1991; *Rohling and Bryden*, 1994]. This model simulates ΔS_{gib} well, but overestimates Q_{med} by a factor of ~1.3 [*Tsimplis and Bryden*, 2000]. Volume transports in our calculations for the deglaciation are therefore based on a modern baseline of 0.67Sv [*Tsimplis and Bryden*, 2000], from which past Q_{med} is calculated according to the quasi-linear relationship 3.91 $\times$ 10^{-4} Sv m^{-1} shown by [*Rohling and Bryden*, 1994].

[11] Changes in the volume of Mediterranean Outflow through the Strait of Gibraltar with changing sea level during the deglaciation were calculated under the assumption that net evaporation from the Mediterranean remained approximately constant through time, which has been found

Figure 2. (a) Location of sediment drifts and cores. (b) Sedimentological and chronostratigraphic information for the Gulf of Cadiz contourite over the last deglaciation. T1a indicates Termination 1a, and YD indicates Younger Dryas. Chronostratigraphy for Kc8227 is derived from biostratigraphy [*Stow et al.*, 1986], and that for the part of MC39008-3 between 10.6 and 18.2 ka is derived from tuning of a $\delta^{18}O_{G.\ bulloides}$ record [*Heilemann*, 2000; *Schönfeld and Zahn*, 2000]. Core N-2 is taken from *Nelson et al.* [1993].

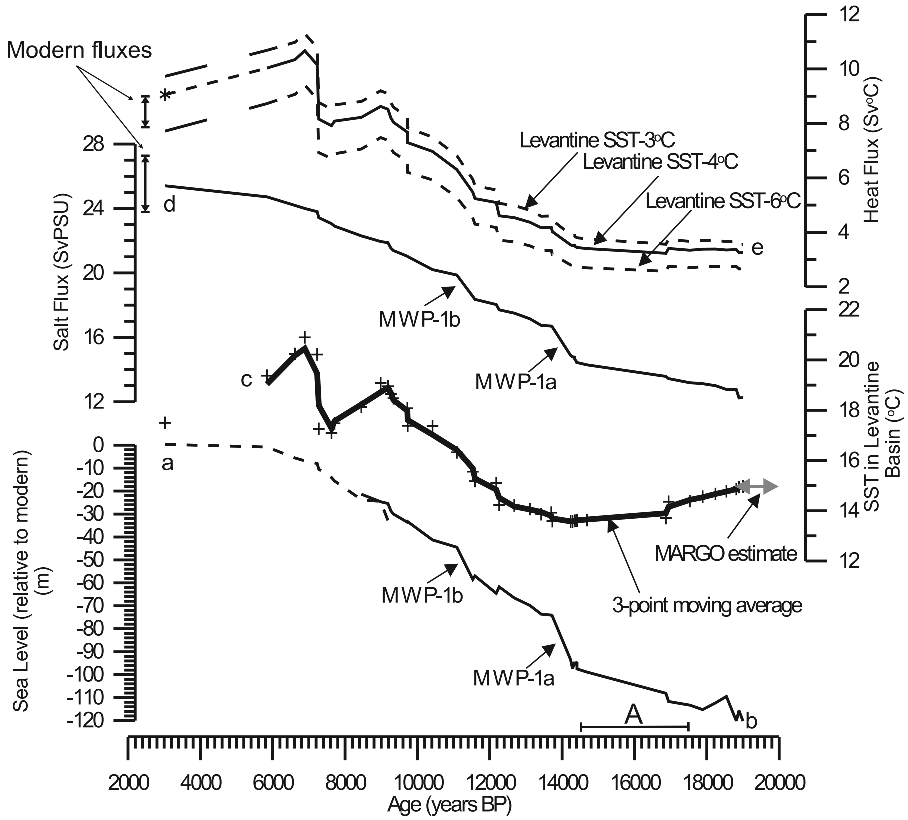

Figure 3. Export fluxes from Mediterranean Sea to eastern North Atlantic: relative sea level for Tahiti [*Bard et al.*, 1996] (line a), relative sea level for Barbados [*Fairbanks*, 1989] (line b), SST from Levantine Basin [*Emeis et al.*, 2000] (line c), Mediterranean Outflow salt flux (line d), and Mediterranean Outflow heat flux (line e). MARGO estimate for Levantine winter SST is taken from *Hayes et al.* [2005]. Modern salt and heat fluxes for the modern MOW are shown as bars on left (estimates taken from measured modern transport and Outflow Water properties [*Tsimplis and Bryden*, 2000]). The period shown as "A" is the time of little or no NADW formation [*McManus et al.*, 2004], as detailed in paragraph 22.

to be reasonable for the LGM [*Bigg*, 1995] and much of the deglaciation [*Matthiesen and Haines*, 2003; *Rohling*, 1999; *Rohling and Bryden*, 1994]. The sea level changes used in our reconstructions rely on the coral-based sea level record for the last deglaciation [*Bard et al.*, 1996; *Fairbanks*, 1989] (Figure 3, lines a and b).

[12] Calculation of the MOW salt flux uses estimates of ΔS_{gib} and the volume flux as obtained from the hydraulic arguments, and the salinity of Atlantic water taking into account the ice volume concentration effect. The global ice volume concentration effect on Atlantic salinity is accounted for according to [*Matthiesen and Haines*, 2003] as

$$S_{atl} = S_{atl}^{present} \frac{H_{Global\ ocean}}{H_{Global\ ocean} - h'} \tag{2}$$

where $S_{atl}^{present}$ = 36 psu, $H_{Global\ ocean}$ = 3800 m and h′ = relative sea level change derived from the coral-based sea level record [*Bard et al.*, 1996; *Fairbanks*, 1989].

[13] MOW heat flux calculations also rely on the volume flux obtained from the hydraulic arguments, together with the estimated temperature of the outflow. Paleo-MOW temperature is estimated from a reconstruction of Levantine Intermediate Water (LIW) temperature. LIW forms in the Levantine Basin during the winter [*Bryden and Stommel*, 1984] and contributes >90% of water exported at Gibraltar today [*Bryden et al.*, 1994]. At sill depth, LIW is ~12.5°C today, 4 to 5°C cooler than winter sea surface temperature (WSST) in the Levantine Basin, due to mixing with cooler Deep Waters [*Bryden et al.*, 1994]. We assume that this offset is approximately stable through time, and thus calculate paleo-LIW temperature from SST records for the Levantine Basin [*Emeis et al.*, 2000]. The SST reconstruction used (Figure 3, line c) employs an alkenone proxy (U-37$^{k'}$) and so may slightly overestimate WSST. However, values for ~19ka B.P. (~15°C) are consistent with independent WSSTs from an Artificial Neural Network reconstruction from planktonic foraminiferal assemblages for the LGM [*Hayes et al.*, 2005] (see Figure 3).

3. Results

[14] Correlation between cores from the Gil Eanes Drift follows that previously published [*Rogerson et al.*, 2005],

slightly modified to take the 8 new AMS^{14}C datings (Table 1) into account. Within these records, the last glacial termination (T1a) is marked by a substantial and abrupt decline in $\delta^{18}O_{planktonic\ foraminifera}$ at approximately 14.6 ka (see Figure 2), which coincides with the reappearance of the warm water planktonic foraminifera *Globigerinoides ruber*, both of which features are widely reported for the region [*Rogerson et al.*, 2005; *Sierro et al.*, 1999]. The Younger Dryas (YD) is characterized by a period of synchronous increase in $\delta^{18}O_{planktonic\ foraminifera}$ and near disappearance of *G. ruber* (immediately subsequent to a radiocarbon dating of 13.5 ka in D13898), which again are regional features [*Rogerson et al.*, 2005; *Sierro et al.*, 1999]. The position of T1a and the YD in M39008-3 are identified on the basis of the same events [*Heilemann*, 2000], and so this record is directly correlatable to the Gil Eanes Drift cores. The position of T1a and the YD in Kc8227 are identified on the basis of biostratigraphy (especially variability in *G. ruber*) alone [*Stow et al.*, 1986]; the regional expression of these events makes their placement reliable, however. The position of events within the N-# cores is approximate, based on the position of radiocarbon datings.

[15] Around 15.0–14.5 ka B.P., changes in the GoC sedimentary system show a remarkable contrast between sites above and below 1000 m water depth. Above 1000 m, there is an onset of sand deposition, following generally muddy deposition during the last glaciation [*Nelson et al.*, 1993]. Three sandy intervals (Peak Contourites I, II and III) mark discrete periods of intensified flow [*Stow et al.*, 1986]. Core M39008-3 shows these to be of deglacial (~15 ka B.P.), Younger Dryas (~12 ka B.P.), and late Holocene (<6.8 ka B.P.) age, respectively [*Heilemann*, 2000; *Schönfeld*, 2002]. On Faro Drift (Figure 2a), Peak Contourite I coincides with the first arrival of warm water planktic foraminifera, placing it at the onset of the Bölling warming [*Stow et al.*, 1986].

[16] Below 1000 m depth, cores D13900 and D13898 show distinct reductions in both grain size and accumulation rate across the last deglaciation (see Figure 2b). D13898, situated on the muddy flank of the Gil Eanes Drift, shows a gradual grain size reduction through the deglaciation that culminates in a grain size minimum around 14.6 ka B.P. (Figure 2b), which suggests a reduction in local current energy. D13900 shows an abrupt decrease in grain size, with the first muddy (>90% finer than 63 μm) deposition appearing around 14.7 ka B.P. As D13900 characterizes the termination of the Gil Eanes Channel (Figure 2a), this observation likely reflects an abrupt increase in the entrainment of sand higher on the slope, rather than a change in local current energy [*Rogerson et al.*, 2005]. D13892 contains 2 periods of increased Fe/Ca ratios that correspond in age to Terminations 1a and 1b (14.6 ka and 11.6 ka B.P. respectively), and which reflect short (~300 year) bursts of increased fine sediment supply.

[17] In the "Sandy Channels" region which spans the 1000 m contour (Figure 2a), the entire interval representing the deglaciation (18–10 ka B.P. [*Boyle*, 2000]) is generally absent, with the oldest preserved sands normally dating to the early Holocene (<10 ka B.P.), although isolated depositional packages are preserved that are of late deglacial age (12.8 ka B.P.) [*Nelson et al.*, 1993]. The deglacial unconformity extends onto the upper Gil Eanes Drift, where it is recorded in cores D13686 and D13896 (Figure 2).

[18] Both salt and heat export from the Mediterranean Sea increased significantly through the last deglaciation in our reconstruction, with distinct "jumps" at times of rapid sea level rise (Figure 3). During the period of interest (18–10 ka B.P.) transport values increase from 13.5 Sv PSU and ~3.3 Sv °C to 20.9 Sv PSU and ~7 Sv °C respectively. At MWP-1a, the salt flux is estimated to have increased by ~2.3 Sv PSU and heat flux by ~0.75 Sv °C.

4. Discussion and Conclusions

[19] The changes in the distribution of sand deposition and net erosion described above indicate that a rapid and significant change occurred in the current pattern on the northern GoC slope between 15 and 14.5 ka B.P. (Figure 1b). Abrupt shoaling of the top of the MOW plume is indicated by an abrupt increase in sand deposition above 1000 m on the slope and virtual cessation of sand deposition below this depth. The development of current activity at the sites of Kc8227 and M39008-3 indicates that the top of the MOW core shoaled to approximately its present depth (~500 m). At the same time, the presence of erosive flow (deglacial unconformity) at D13896 (see Figure 2) indicates that the base of the plume descended more rapidly than it does today, and reached greater depths (>1500 m), in agreement with evidence from the Portuguese margin [*Schönfeld and Zahn*, 2000]. The abrupt increase in the dominance of the detrital phase in D13892 indicates that the supply of suspended sediment to this location by the MOW was also significantly enhanced during this period [*Rogerson et al.*, 2006], indicating significant activity in the lower part of the plume and/or a significant increase in its internal turbulence. Combined, this indicates that the MOW plume had intensified and extended over an increased depth range around 15.0–14.5 ka B.P. (Peak Contourite I; Figure 1b). A similar, if less intense, flow pattern developed during the Younger Dryas (Peak Contourite II). During the period 14–13 ka B.P. between Peak Contourites I and II, there are no indications of strong flow in any of the records (Figure 2b). Presumably, the core of the MOW plume at that time resided within the depth range of the deglacial unconformity (600–1000 m on the cross sections shown in Figure 1), which would imply that it remained at an intermediate position between its glacial and interglacial positions (Table 3).

[20] Though the suggestion that the MOW penetrates north of the Scotland-Greenland Ridge and directly influences surface conditions in the Nordic seas [*Reid*, 1979] is no longer widely accepted [*Bower et al.*, 2002; *Hill and Mitchelson-Jacob*, 1993], it is likely that Mediterranean-derived salt is supplied directly to sites of North Atlantic Intermediate Water formation (south of Greenland), and indirectly, via vertical mixing, to the Nordic Seas [*McCartney and Mauritzen*, 2001]. Reductions in North Atlantic Deep Water formation of 1–2 Sv have been suggested from a global circulation model with a dammed

Table 3. Activity of the MOW Through Time[a]

	N-1 (~500 m)	N-2 (~500 m)	M39008-3 (577 m)	N-3 (~600 m)	Kc8227 (619 m)	D13896 (817 m)	D13686 (998 m)	D13898 (1111 m)	D13900 (1297 m)	D13892 (1514 m)
LGM	inactive	inactive	inactive	inactive	inactive	active	active	active	active	low supply
T1a	erosive	erosive	active	erosive	active	erosive	erosive	reducing	reducing	high supply
B-A	erosive	erosive	inactive		inactive	active	erosive	inactive	inactive	low supply
YD + T1b	erosive	erosive	active	inactive	active	erosive	erosive	active	active	high supply
Early Holocene[b]	?	?	low activity[b]	?	low activity[b]	?	erosive	minimal activity/ inactive (base)	inactive	low supply
Late Holocene	active (top)	active (top)	active (top)	active (top)	active (top)	active (core)	active (base)	minimal activity/ inactive (base)	inactive	low supply

[a]Core records are arranged in order of depth increasing from left to right. Inference of MOW activity is made on the basis of whether the sediment is dominantly sand (MOW active) or mud (MOW inactive), and it should be noted that very low velocity flow (<~0.1 m s^{-1}) is not distinguished from MOW inactive. Words in parentheses indicate which part of the MOW plume is active at each location today. Activity for D13892 is inferred on the basis of the supply of detrital sediment interpreted from the Fe/Ca record.

[b]May reflect reduced export of Mediterranean water during time of sapropel S1.

Strait of Gibraltar [*Rahmstorf*, 1998], even though that model was of insufficient resolution to produce a well-defined MOW plume [*Thorpe and Bigg*, 2000] (it assumed only diffusive mixing from a point source in the Gulf of Cadiz [*Rahmstorf*, 1998]). Shoaling of the MOW plume's top and increases in its salt flux, as described here to have happened gradually throughout the deglaciation (with particular "jumps" around 15.0–14.5 ka B.P. and around the Younger Dryas), would therefore substantially enhance its potential to affect downwelling both south of Greenland and within the Nordic Seas. As both MOW volume and salt flux increase strongly in proportion with sea level rise [*Rohling and Bryden*, 1994], the MOW forms a strong candidate for the density amplification in the North Atlantic that would be required to maintain North Atlantic Deep Water formation through times of rapid large-scale glacial retreat [*Schmidt et al.*, 2004], such as MWP-1a around 14.2 ka B.P. (Figure 3, line d).

[21] Although the sea level change related accelerations in MOW volume and salt flux are most conspicuous in Figure 3 (line d), we here emphasize the gradual MOW increase during the earlier part of the deglaciation, and especially its abrupt shoaling around 15.0–14.5 ka B.P., because these processes may have (partially) controlled the abrupt MOC resumption around 14.6 ka B.P. [*Gherardi et al.*, 2005; *McManus et al.*, 2004].

[22] Net export of fresh water to the Indian Ocean catchment leads to enhanced salinity in the Mediterranean and, consequently, throughout the North Atlantic to the north of 25°N [*Bryden and Stommel*, 1982]. The rate of net fresh water export from the Mediterranean is expected to be about 0.046 Sv between 17.5 and 14.5 ka B.P., a period that was characterized by virtual cessation of North Atlantic deep and intermediate water formation [*Gherardi et al.*, 2005; *McManus et al.*, 2004]. With very limited export of deep or intermediate water from the North Atlantic for about 3 ka, the integrated MOW salt flux would cause a mean salinity increase in the North Atlantic. If we consider that this impact would be evenly distributed over the upper 2000 m of the entire North Atlantic to the north of 25°N (including the Nordic Seas up to 80°N and Labrador Sea up to 65°N), this impact can be estimated on the basis of the proportional loss of volume incurred when subtracting the integrated export of freshwater between 17.5 and 14.5 ka B.P. from the modern water volume,

$$\Delta S_{atl} = \frac{Q_F C \Delta t}{V_{atl}} \mathrm{S_{atl}} \qquad (3)$$

Here ΔS_{atl} is the change in salinity of the region specified; S_{atl} is obtained from equation (2); Q_F is the freshwater flux ($Q_{atl} - Q_{med}$) obtained from equation (1) and under the assumed stable net evaporation rate is constant at ~0.046 Sv; C is the number of seconds per year; Δt is the duration of the time period specified (3000 years); and V_{atl} is the volume of the region specified, based on the ETOPO5 database (4×10^{16} m^3) [*National Geophysical Data Center*, 1988]. This simple calculation indicates that continued MOW influx at a time (17.5–14.5 ka B.P.) of very limited export of deep or intermediate water from the North Atlantic would suffice to cause a mean salinity increase ~0.5 psu (a density change of ~0.4 kg m^{-3}) throughout the upper 2000 m of the entire North Atlantic to the north of 25°N.

[23] Given the reconstructed depth range and the geographic location of the MOW plume prior to shoaling at 14.6 ka, this influence would have been focused at 1000–2000 m depth in the northeastern North Atlantic. There is observational support for this expected salt accumulation in the form of a gradual increase of ~0.15‰ kyr^{-1} in $\delta^{18}O_{sea\ water}$ in NE Atlantic intermediate water (1627 m depth, 61.30°N, 24.11°W), starting around 16.5 ka B.P. [*Rickaby and Elderfield*, 2005]. The inferred salt accumulation within the North Atlantic between about 17.5 and 14.5 ka B.P. would have provided an important preconditioning for abrupt resumption of intermediate and deep overturning around 14.6 ka B.P. [*Gherardi et al.*, 2005; *McManus et al.*, 2004]. Moreover, the abrupt shoaling of the MOW plume to its present depth range around 15.0–14.5 ka B.P. would likely have reversed the potential density relationship between Glacial North Atlantic and Antarctic Intermediate Waters, which is considered critical for a resumption of the MOC [*Rickaby and Elderfield*, 2005].

[24] **Acknowledgments.** We thank S. Cooke, M. Cooper, and M. Bolshaw for their invaluable assistance in stable isotope mass spectrometry, Guy Rothwell and Ian Croudace for their assistance during

XRF logging, and Bob Marsh for kindly providing volumetric data from the North Atlantic. We would also like to thank Fransisco Sierro and Gerald Dickens for their constructive reviews. The 19 "old" radiocarbon datings were carried out as part of NERC-RCL project 949.1201.

References

Bard, E., et al. (1996), Deglacial sea-level record from Tahiti corals and the timing of global meltwater discharge, *Nature*, *382*, 241–244.

Bard, E., et al. (1998), Radiocarbon calibration by means of mass spectrometric ^{230}Th/^{234}U and ^{14}C ages of corals: An updated database including samples from Barbados, Mururoa and Tahiti, *Radiocarbon*, *40*, 1085–1092.

Bigg, G. R. (1995), Aridity of the Mediterranean Sea at the Last Glacial Maximum: A reinterpretation of the δ^{18}O record, *Paleoceanography*, *10*, 283–290.

Bower, A. S., et al. (2002), Directly measured mid-depth circulation in the northeastern North Atlantic Ocean, *Nature*, *419*, 603–607.

Boyle, E. A. (2000), Is ocean thermohaline circulation linked to abrupt stadial/interstadial transitions?, *Quat. Sci. Rev.*, *19*, 255–272.

Bryden, H. L., and T. Kinder (1991), Steady two-layer exchange through the Strait of Gibraltar, *Deep Sea Res., Part A*, *38*, S445–S463.

Bryden, H. L., and H. M. Stommel (1982), Origins of the Mediterranean Outflow, *J. Mar. Res.*, *40*, 55–71.

Bryden, H. L., and H. M. Stommel (1984), Limiting processes that determine basic features of the circulation in the Mediterranean Sea, *Oceanol. Acta*, *7*, 289–296.

Bryden, H. L., et al. (1994), Exchange through the Strait of Gibraltar, *Prog. Oceanogr.*, *33*, 201–248.

Cacho, I., et al. (2001), Variability of the western Mediterranean Sea surface temperature during the last 25,000 years and its connection with the Northern Hemisphere climatic changes, *Paleoceanography*, *16*, 40–52.

Coplen, T. B. (1994), Reporting of stable hydrogen, carbon, and oxygen isotopic abundances, *Pure Appl. Chem.*, *66*, 273–276.

Emeis, K.-C., et al. (2000), Temperature and salinity variations of Mediterranean Sea surface waters over the last 16,000 years from records of planktonic stable oxygen isotopes and alkenone unsaturation ratios, *Palaeogeogr. Palaeoclimatol. Palaeoecol.*, *158*, 259–280.

Fairbanks, R. G. (1989), A 17,000-year glacio-eustatic sea-level record—Influence of glacial melting rates on the Younger Dryas event and deep-ocean circulation, *Nature*, *342*, 637–642.

Gherardi, J.-M., et al. (2005), Evidence from the northeastern Atlantic basin for variability in the rate of meridional overturning circulation through the last deglaciation, *Earth Planet. Sci. Lett.*, *240*, 710–723.

Hayes, A., et al. (2005), Glacial Mediterranean sea surface temperatures based on planktonic foraminiferal assemblages, *Quat. Sci. Rev.*, *24*, 999–1016.

Heilemann, K. (2000), Hydrodynamische Änderungen des Mittelmeerausstromwassers und Deren Abbildung in den Sedimenten des Iberischen Kontinentalhangs, Ph.D. thesis, 116 pp., Christian-Albrechts-Univ., Kiel, Kiel, Germany.

Hill, A. E., and E. G. Mitchelson-Jacob (1993), Observations of a poleward-flowing saline core on the continental slope west of Scotland, *Deep Sea Res., Part I*, *40*, 1521–1527.

Knorr, G., and G. Lohmann (2003), Southern Ocean origin for resumption of Atlantic thermohaline circulation during deglaciation, *Nature*, *424*, 532–536.

Matthiesen, S., and K. Haines (2003), A hydraulic box model study of the Mediterranean response to postglacial sea-level rise, *Paleoceanography*, *18*(4), 1084, doi:10.1029/2003PA000880.

McCartney, M. S., and C. Mauritzen (2001), On the origin of the warm inflow to the Nordic Seas, *Prog. Oceanogr.*, *51*, 125–214.

McManus, J. F., et al. (2004), Collapse and rapid resumption of Atlantic meridional circulation linked to deglacial climate changes, *Nature*, *428*, 834–837.

National Geophysical Data Center (1988), Data Announcement MGG-02, Digital Relief of the Surface of the Earth, http://www.ngdc.noaa.gov/mgg/fliers/93mgg01.html, NOAA, Boulder, Colo.

Nelson, C. H., et al. (1993), Mediterranean undercurrent sandy contourites, Gulf of Cadiz, Spain, *Sediment. Geol.*, *82*, 103–131.

O'Neill-Baringer, M., and J. F. Price (1999), A review of the physical oceanography of the Mediterranean outflow, *Mar. Geol.*, *155*, 63–82.

Rahmstorf, S. (1998), Influence of Mediterranean Outflow on climate, *Eos Trans. AGU*, *79*(24), 281–282.

Reid, J. L. (1979), On the contribution of the Mediterranean Sea outflow to the Norwegian-Greenland Sea, *Deep Sea Res., Part A*, *26*, 1199–1223.

Rickaby, R. E. M., and H. Elderfield (2005), Evidence from the high-latitude North Atlantic for variations in Antarctic Intermediate Water flow during the last deglaciation, *Geochem. Geophys. Geosyst.*, *6*, Q05001, doi:10.1029/2004GC000858.

Rogerson, M., E. J. Rohling, P. P. E. Weaver, and J. W. Murray (2005), Glacial to interglacial changes in the settling depth of the Mediterranean Outflow plume, *Paleoceanography*, *20*, PA3007, doi:10.1029/2004PA001106.

Rogerson, M., et al. (2006), Colour logging as a tool in high-resolution palaeoceanography, in *New Ways of Looking at Sediment Cores and Core Data*, edited by R. G. Rothwell, *Geol. Soc. Spec. Publ.*, in press.

Rohling, E. J. (1999), Environmental control on Mediterranean salinity and δ^{18}O, *Paleoceanography*, *14*, 706–715.

Rohling, E. J., and H. L. Bryden (1994), Estimating past changes in the eastern Mediterranean freshwater budget, using reconstructions of sea level and hydrography, *Proc. K. Ned. Akad. Wet, Ser. B*, *97*, 201–217.

Schmidt, M. W., et al. (2004), Links between salinity variation in the Caribbean and North Atlantic thermohaline circulation, *Nature*, *428*, 160–163.

Schönfeld, J. (2002), A new benthic foraminiferal proxy for near-bottom current velocities in the Gulf of Cadiz, northeastern Atlantic Ocean, *Deep Sea Res., Part I*, *49*, 1853–1875.

Schönfeld, J., and R. Zahn (2000), Late glacial to Holocene history of the Mediterranean Outflow: Evidence from benthic foraminiferal assemblages and stable isotopes at the Portuguese margin, *Palaeogeogr. Palaeoclimatol. Palaeoecol.*, *159*, 85–111.

Sierro, F. J., et al. (1999), Late glacial to recent palaeoenvironmental changes in the Gulf of Cadiz and formation of sandy contourite layers, *Mar. Geol.*, *155*, 157–172.

Stow, D. A. V., et al. (1986), Facies distribution and textural variation in Faro Drift contourites: Velocity fluctuation and drift growth, *Mar. Geol.*, *72*, 71–100.

Thorpe, R. B., and G. R. Bigg (2000), Modelling the sensitivity of Mediterranean Outflow to anthropogenically forced climate change, *Clim. Dyn.*, *16*, 355–368.

Tsimplis, M. N., and H. L. Bryden (2000), Estimation of the transports through the Strait of Gibraltar, *Deep Sea Res., Part I*, *47*, 2219–2242.

Weltje, G. J., and M. A. Prins (2003), Muddled or mixed? Inferring palaeoclimate from size distributions of deep-sea clastics, *Sediment. Geol.*, *162*, 39–62.

M. Rogerson, Geography Department, University of Hull, Cottingham Road, Hull HU6 7RX, UK. (m.rogerson@hull.ac.uk)

E. J. Rohling and P. P. E Weaver, National Oceanography Centre, Southampton, European Way, Southampton SO14 3ZH, UK.